

# Enhanced Optical Nonlinearity in Noncovalently Functionalized Amphiphilic Graphene Composites

Tingchao He,<sup>[a]</sup> Xiaoying Qi,<sup>[b]</sup> Rui Chen,<sup>[a]</sup> Jun Wei,<sup>[b]</sup> Hua Zhang,<sup>\*,[c]</sup> and Handong Sun<sup>\*,[a]</sup>

The good solubility of graphene-based materials in various solvents without sacrificing their intrinsic properties is a prerequisite for their further applications. In particular, it is important for application as a practical optical limiter. A comprehensive study was conducted on the nonlinear optical property of a rationally designed amphiphilic graphene composite (PEG-OPE-rGO). By taking advantages of the unique energy diagram of this graphene composite, the optical limiting (OL) performances of PEG-OPE-rGO, which is either dissolved in solvents with moderate polarity or fabricated into thin solid films, are

beyond the reported results for other graphene composites. Importantly, the main factors for the enhanced OL response of PEG-OPE-rGO are the multiphoton absorption and Förster resonance energy transfer process, instead of the nonlinear scattering mechanism observed for common nanostructured materials. The excellent OL response of PEG-OPE-rGO allows it to be one of the best candidates in practical optical limiters. Moreover, the mechanism analysis provides the deep insight for further optimization of the design of promising OL materials.

## Introduction

In the past decades, there has been great progress in development of organic and inorganic optical limiters with large nonlinear optical (NLO) response. Carbon-based materials, including carbon black suspension (CBS),<sup>[1]</sup> single- and multi-walled carbon nanotubes (CNTs),<sup>[2,3]</sup> and some small  $\pi$ -electron systems, such as fullerenes,<sup>[4]</sup> porphyrins, and phthalocyanines<sup>[5]</sup> have been widely explored as advanced optical limiters. For example, the thermally induced nonlinear scattering of CBS and CNTs is generally accepted as the principal mechanism for the optical limiting (OL).<sup>[1-3]</sup> As known, the OL effect of graphitic systems covers a broad wavelength, ranging from the visible to near infrared. However, good OL behavior of graphitic systems only performs in solution, owing to the dominance of scattering mechanism. The solution-assisted performance is a serious obstacle for practical applications, as the graphitic system tends to aggregate into large bundles because of its relatively high surface energy. Therefore, more research interests have been directed towards the development of graphitic materials which have good dispersability and can be processed in liquid dispersion. It was reported that the small  $\pi$ -electron systems can be homogeneously dispersed in solution or solid phases, showing good OL properties in the sub-nanosecond timescale.<sup>[4]</sup> Unfortunately, these systems only have a narrow band OL behavior as the ratio of excited state to ground state cross section strongly depends on the excitation wavelength.<sup>[6]</sup> For example, C<sub>60</sub> has very poor OL properties beyond 700 nm, which cannot meet the requirement of OL devices for sensor protection, because band protection for the entire operating wavelength of the sensor system is required.

Graphene, as the newly explored single-layer carbon material, is found to be a promising broadband optical limiter owing to the strong nonlinear scattering mechanism.<sup>[7]</sup> Moreover, the enhanced OL behaviors have been reported in graphene

hybrid materials covalently functionalized with porphyrin,<sup>[8]</sup> organic dye ionic complex,<sup>[9]</sup> oligothiophene,<sup>[10]</sup> fullerene,<sup>[11]</sup> phthalocyanine,<sup>[12]</sup> upconversion rare-earth nanoparticles,<sup>[13]</sup> and poly(*N*-vinylcarbazole).<sup>[14]</sup> However, the poor solubility of these graphene hybrid materials is one of the big problems limiting their practical application. Although covalent functionalization was used to improve the solubility of graphene hybrid materials, it is a destructive method that may alter the chemical structures of graphene and its derivatives, such as graphene oxide (GO) and reduced graphene oxide (rGO).

To maintain the intrinsic property of graphene, an alternative method that can protect the basic plane of graphene is preferred. Moreover, on one hand, the good thermal conductivity of graphene is beneficial to the excellent OL response. On the other hand, graphene is an innate energy acceptor, and its OL behavior can be enhanced by functionalization with nonlinear optical chromophores (donors), which can promote the energy transfer between them. Therefore, the noncovalent functionalization of graphene with amphiphilic conjugated molecules,

[a] T. He, R. Chen, Prof. H. Sun  
Division of Physics and Applied Physics  
School of Physical and Mathematical Sciences  
Nanyang Technological University  
Singapore 637371 (Singapore)  
E-mail: hdsun@ntu.edu.sg

[b] Dr. X. Qi, Dr. J. Wei  
Singapore Institute of Manufacturing Technology  
71 Nanyang Drive, Singapore 638075 (Singapore)

[c] Prof. H. Zhang  
School of Materials Science and Engineering  
Nanyang Technological University  
50 Nanyang Avenue, Singapore 639798 (Singapore)  
E-mail: hzhang@ntu.edu.sg  
Homepage: <http://www.ntu.edu.sg/home/hzhang/>

through the nondestructive  $\pi$ - $\pi$  interactions, could be a simple fabrication method to sufficiently combine the properties of individual components, endue the high solubility to graphene (or GO), and maintain the intrinsic property of graphene.<sup>[15]</sup> Recently, our research group synthesized an amphiphilic graphene composite (PEG-OPE-rGO; PEG = poly(ethylene glycol), OPE = oligo(phenylene ethynylene), rGO = reduced graphene oxide),<sup>[16]</sup> in which the coil-rod-coil conjugated triblock copolymer (PEG-OPE) was used to functionalize the graphene and provide the super dispensability in a variety of solvents, ranging from the low polar toluene to high polar water. Herein, we present a systematic study on the NLO properties of PEG-OPE-rGO—its super dispensability advances are beneficial in the application of OL devices. Our experimental results show that the PEG-OPE-rGO exhibits excellent broadband OL response not only in polar/nonpolar solvent but also in thin solid films, thus indicating that it is an excellent candidate for the optical limiter.

## Results and Discussion

### Linear optical properties

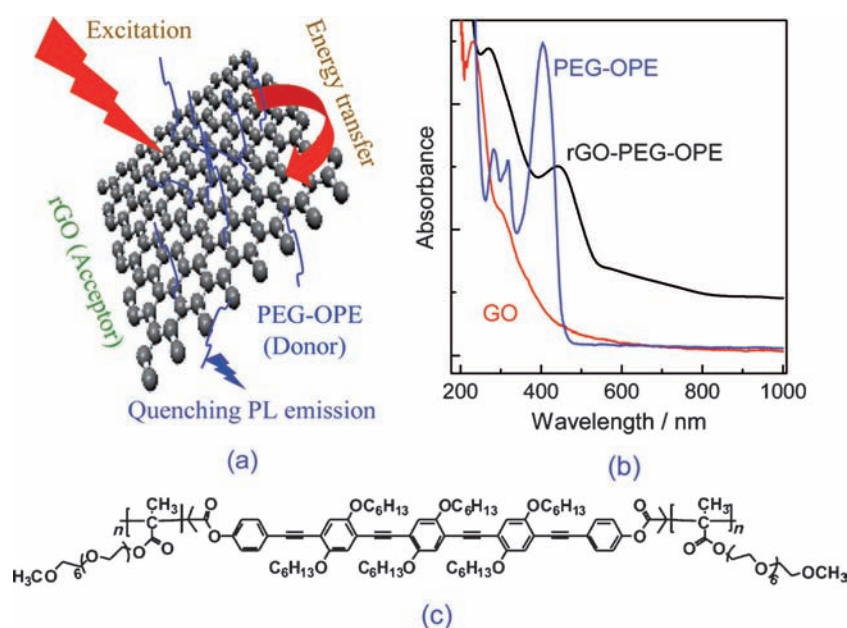
Scheme 1 a shows the schematic diagram of energy transfer in the PEG-OPE-rGO composite. The synthesized PEG-OPE-rGO can be well dispersed in a variety of solvents. The detailed characterization of this amphiphilic graphene composite was published elsewhere.<sup>[16]</sup> To facilitate the investigation of its nonlinear optical property, we first present the linear optical property of PEG-OPE-rGO and analyze the corresponding physical mechanism. Scheme 1 b shows the UV/Vis absorption spectra of GO, PEG-OPE, and PEG-OPE-rGO in  $\text{CHCl}_3$ . The absorption

band at 228 nm in GO is assigned to the  $\pi$ - $\pi^*$  transition of the C=C bonds, meanwhile the appearance of the shoulder at 304 nm corresponds to the  $n$ - $\pi^*$  transitions.<sup>[17]</sup> As for the PEG-OPE-rGO composite, the absorption band of GO shifted from 229 to 272 nm, indicating the reduction of GO to rGO,<sup>[18]</sup> meanwhile the band corresponding to PEG-OPE shifted from 403 to 450 nm, indicating that there is greatly extended  $\pi$ -conjugation of PEG-OPE in the presence of rGO.<sup>[16,18,19]</sup> Moreover, as compared with GO and PEG-OPE, the absorption band of PEG-OPE-rGO became much broader in the whole spectroscopic region, thus suggesting the appearance of strong electronic interaction between rGO and PEG-OPE in the ground state as a result of  $\pi$ - $\pi$  stacking. The dramatic changes in UV/Vis absorption spectra indicate it is possible to obtain a different nonlinear optical property from PEG-OPE-rGO. The molecular structure of PEG-OPE is shown in Scheme 1 c. It is expected that the symmetric molecular structure along with  $\pi$ -conjugated oligomer can provide the high multiphoton absorption cross-section,<sup>[20]</sup> which is beneficial to the enhancement of OL response in PEG-OPE-rGO.

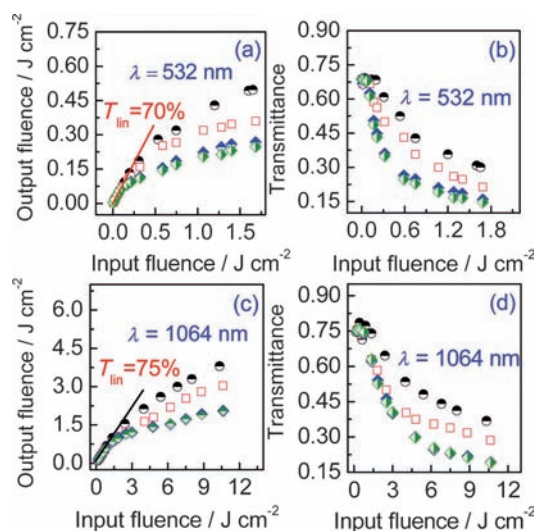
### Nonlinear optical properties in solutions

Figure 1 a,c show the OL curves of GO in ethanol and PEG-OPE-rGO in various solvents with different polarities under the excitation of 532 nm. All of the samples were adjusted to have the same linear transmittance of 70%. At lower incident input fluence, there was no significant change in the transmittance. However, their transmittance started to decrease when the input fluence increased beyond a certain threshold (onset of OL). The OL threshold, defined as the input power density at which the transmission falls to 50% of the linear transmittance, varies for the different samples.

At the highest input fluence used in this study, the output fluences for a solution of GO in ethanol, and PEG-OPE-rGO in ethanol,  $\text{CHCl}_3$ , and  $\text{CS}_2$  are 0.51, 0.36, 0.27, and 0.25  $\text{J cm}^{-2}$ , respectively, and the corresponding OL thresholds are 1.19, 0.75, 0.35, and 0.31  $\text{J cm}^{-2}$ , respectively. The OL curves obtained under the excitation of 1064 nm are presented in Figure 1 b,d, from which the corresponding OL thresholds are determined to be 10.32, 4.80, 3.52, and 3.50  $\text{J cm}^{-2}$ , respectively. Obviously, under the excitation of both 532 and 1064 nm, the PEG-OPE-rGO composite displays an improved OL behavior compared with GO. Moreover, it is noteworthy that PEG-OPE-rGO in  $\text{CHCl}_3$  or  $\text{CS}_2$  displays one of lowest OL thresholds compared to those reported



**Scheme 1.** a) Schematic diagram of energy transfer in the PEG-OPE-rGO composite. b) UV/Vis absorption spectra of GO, PEG-OPE, and PEG-OPE-rGO in ethanol. c) Molecular structure of the amphiphilic coil-rod-coil conjugated triblock copolymer (PEG-OPE).



**Figure 1.** Measured output fluence and nonlinear transmission versus input fluence for GO in ethanol and PEG-OPE-rGO in various solvents (ethanol,  $\text{CHCl}_3$ , and  $\text{CS}_2$ ) under the excitation of (a,b) 532 nm and (c,d) 1064 nm. Note: ● represents GO in ethanol; □ represents PEG-OPE-rGO in ethanol; ◆ represents PEG-OPE-rGO in  $\text{CHCl}_3$ ; ◇ represents PEG-OPE-rGO in  $\text{CS}_2$ .

previously.<sup>[11,21]</sup> Therefore, PEG-OPE-rGO has potential application in the broadband optical limiter.

Until now, mechanisms, including the nonlinear scattering (NLS) and nonlinear absorption,<sup>[22,23]</sup> have been proposed for the OL effect. Nonlinear scattering is the energy-spreading type of OL mechanism, meanwhile nonlinear absorption is the energy-absorbing-type of OL mechanism. Although the NLS mechanism has already been studied in the nanostructured materials,<sup>[8–12]</sup> it is still necessary to measure the NSL signal in the new system to further investigate the detailed OL mechanisms. To explore this nonlinear mechanism, we collected a fraction of scattering light at a forward planar angle of  $20^\circ$ . As shown in Figure 2a,b, at 532 and 1064 nm the scattered light intensity increased significantly with increasing the input optical intensity. It proved that NLS played an important role in the OL. Moreover, the onset of decrease of transmittance was in accordance with the growth of the scattered light, which further confirmed that NLS was relevant to the OL effect. In the nanosecond regime, the strong NLS of GO and PEG-OPE-rGO should arise from the strong scattering centers consisting of the ionized carbon microplasmas and solvent microbubbles. Figure 2c,d shows at 532 or 1064 nm the scattering signals for GO and PEG-OPE-rGO at different angles with respect to the transmitted laser beam, which were measured at the highest fluence used in OL measurements. It was found that at both 532 and 1064 nm, the scattering signals of PEG-OPE-rGO in all solvents were much stronger than those of GO in both forward and backward scattering.

It is well known that the surface tension, viscosity, polarity, and boiling point can affect the nonlinear scattering behavior of solution, that is, the OL response.<sup>[24]</sup> The lower boiling point, smaller surface tension, and lower viscosity lead to better OL performance when the NLS mechanism is dominated. Here,

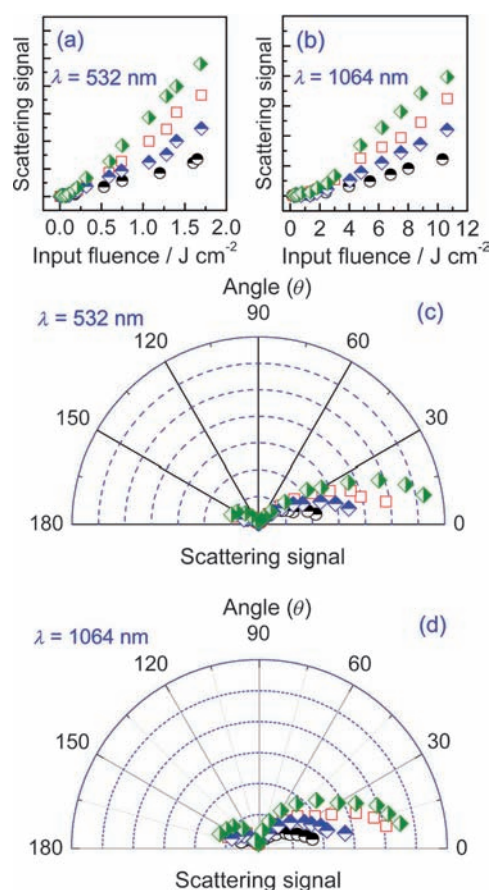


**Figure 2.** Intensity-dependent scattering signals under the excitation of (a) 532 and (b) 1064 nm. Angular-dependent scattering signals under the excitation of (c) 532 and (d) 1064 nm. Note: ● represents GO in ethanol; □ represents PEG-OPE-rGO in ethanol; ◆ represents PEG-OPE-rGO in  $\text{CHCl}_3$ ; ◇ represents PEG-OPE-rGO in  $\text{CS}_2$ .

the dominance of surface tension effect of solvents could be excluded because the OL thresholds did not follow the order of surface tension, that is, ethanol ( $22.1 \text{ mN m}^{-1}$ ) <  $\text{CHCl}_3$  ( $27.2 \text{ mN m}^{-1}$ ) <  $\text{CS}_2$  ( $32.3 \text{ mN m}^{-1}$ ).<sup>[25]</sup> The boiling point of solvent, that is, ethanol ( $78.5^\circ\text{C}$ ) >  $\text{CHCl}_3$  ( $61.7^\circ\text{C}$ ) >  $\text{CS}_2$  ( $46.3^\circ\text{C}$ ), strongly affects the OL behavior of solution, but it should be noted that the OL performance of  $\text{CHCl}_3$  solution is comparable to that of  $\text{CS}_2$  solution. Thus, the influence of boiling point is also excluded. Moreover, in Figure 2, it can be seen that scattering signals in  $\text{CHCl}_3$  are much weaker than those in  $\text{CS}_2$  under 532 or 1064 nm. Therefore, besides the nonlinear scattering mechanism, some other mechanisms might also give important contributions to the OL response of PEG-OPE-rGO. Considering the highly delocalized  $\pi$ -electron system of PEG-OPE, the multiphoton absorption of PEG-OPE may contribute to the enhanced optical nonlinearity in the composite.<sup>[26]</sup> And it has been proved that multiphoton absorption of some molecules strongly depends on the solvent polarity.<sup>[27]</sup> In Figure 2, the dependence of OL response on the solvent polarity was indicated by the presence of stronger multiphoton absorption of PEG-OPE-rGO in some moderately polar solvents, such as in  $\text{CHCl}_3$ .

## Femtosecond time-resolved photoluminescence dynamics

The electronic interaction of PEG-OPE and rGO in the excited state was investigated by using photoluminescence (PL) measurements to understand the mechanism of OL response in PEG-OPE-rGO. Upon excitation at 325 nm, the PL emission of PEG-OPE at 450 and 470 nm was significantly quenched in all the solvents. For example, the PL emission from PEG-OPE-rGO in  $\text{CHCl}_3$  was quenched by 96%, as shown in Figure 3a. The ef-

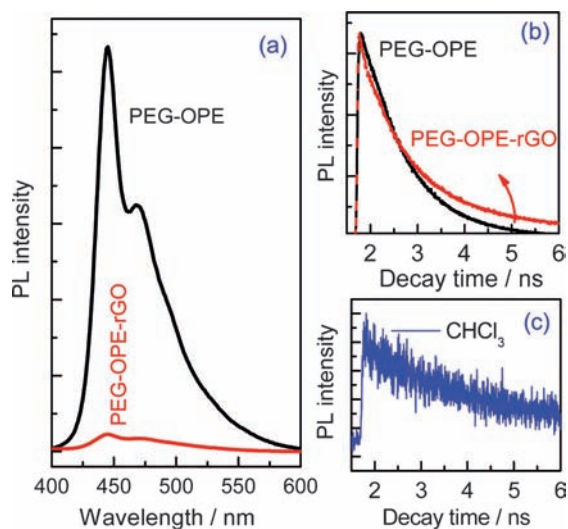


**Figure 3.** a) PL spectra for PEG-OPE-rGO and PEG-OPE in  $\text{CHCl}_3$  under continuous excitation at 325 nm by a He–Cd laser. b) Room temperature TRPL measurements of PEG-OPE and PEG-OPE-rGO in  $\text{CHCl}_3$ . c) Room temperature TRPL measurement of pure  $\text{CHCl}_3$ .

fective emission quenching of PEG-OPE is an indication of electronic interaction between the singlet excited state of the PEG-OPE and rGO. In the PEG-OPE-rGO, PEG-OPE was immobilized on the both sides of rGO sheet, forming a sandwich-like structure.<sup>[16]</sup> PEG-OPE acts as an energy-absorbing and electron-transporting antennae, meanwhile rGO plays the role of electron acceptor. Accordingly, the electron and/or energy transfer from PEG-OPE to rGO in the excited states should enhance the OL behavior in the composite. To further confirm the electronic communication in the excited states of PEG-OPE and rGO, the PL decay dynamics was studied by time-resolved photoluminescence (TRPL) measurements. TRPL was carried out at room temperature by time-correlated single photon counting (TCSPC) under the excitation of 100 fs pulse laser at 350 nm. All the data were monitored under the emission band at 450 nm. The decay of time-dependent PL intensity,  $y(t)$ , as shown in Figure 3b, was well fitted by a biexponential decay with<sup>[28]</sup> Equation (1):

$$y(t) = A_1 \exp(-t/\tau_1) + A_2 \exp(-t/\tau_2) \quad (1)$$

where  $t_1$  and  $t_2$  are two decay times with the respective intensity weights  $A_1$  and  $A_2$ . For PEG-OPE and PEG-OPE-rGO, the ob-

tained data are  $A_1 = 11351$ ,  $\tau_1 \approx 0.86$  ns,  $A_2 = 740$ ,  $\tau_2 = 1.65$  ns and  $A_1 = 7761$ ,  $\tau_1 \approx 0.80$  ns,  $A_2 = 2400$ ,  $\tau_2 \approx 2.96$  ns, respectively. The shorter decay time was ascribed to the PEG-OPE while the longer one resulted from the influence of solvent ( $\text{CHCl}_3$ ), which was further confirmed by the measurement of lifetime of pure solvent ( $A = 48$  and  $\tau \approx 3.36$  ns), as shown in Figure 3c. The influence of solvent to the overall lifetime of PEG-OPE-rGO increased because of the greatly quenched photons emitting from the PEG-OPE, thus resulting in the increased longer decay time (from 1.65 to 2.96 ns). The reduced lifetime of PEG-OPE indicated that the dominant quenching process was caused by the Förster resonance energy transfer (FRET).<sup>[29]</sup> This process produced a charge-separated excited state under the strong pulse excitation. The involvement of the higher excited states led to the enlarged nonlinear absorption and decreased OL threshold.

It is also reported that the extended  $\pi$ -conjugation and defects play an important role in the OL behavior.<sup>[30]</sup> Compared with rGO, the  $\pi$ -conjugation of GO is decreased owing to the existence of many functional groups, such as carboxylic acid and phenolic hydroxy groups.<sup>[31]</sup> Because the PEG-OPE-rGO composite was obtained after the reduction of GO in the presence of PEG-OPE, the  $\pi$ -conjugation in the PEG-OPE-rGO composite was increased by removing functional groups. Meanwhile, rGO can transfer the crystal lattice vibration more rapidly, that is, the thermal conductivity of the PEG-OPE-rGO composite increases. The increase of  $\pi$ -conjugation and thermal conductivity also enhanced the OL property.

## Nonlinear optical property in solid films

In previous reports, the covalently functionalized graphene hybrid materials can only be dissolved in some special solvents.<sup>[8–12]</sup> Therefore, it is difficult to obtain homogenous films for their practical applications. The excellent solubility of PEG-OPE-rGO in various solvents makes it highly feasible for fabrication of homogenous films. In the following part, we will demonstrate the OL behavior of the PEG-OPE-rGO dispersed in the poly(methyl methacrylate, PMMA) matrix at a weight ratio of 2.9% by using the spin-coating method. The obtained film exhibits high transparency (inset in Figure 4a). Figure 4 displays the OL response at 532 and 1064 nm of the cast film. The data were extracted from the open-aperture Z-scan measurements.<sup>[32]</sup> Meanwhile, the damage threshold of the solid film was recorded. When the incident fluence was increased up to  $15.01 \text{ J cm}^{-2}$ , no obvious damage occurred in the solid film, thus indicating the large damage threshold of the prepared film. The film exhibited high linear transmittance at lower input fluence, and the transmittance decreased at higher input fluence, displaying an OL activity with a threshold of  $0.65 \text{ J cm}^{-2}$  at 532 nm and  $6.50 \text{ J cm}^{-2}$  at 1064 nm. As a control experiment, the OL curve of the pure PMMA film under the same experimental conditions was also measured, and gave negligible nonlinearity compared to the cast film. Obviously, the PEG-OPE-rGO offered the major contribution to the OL behavior in the cast film. In addition, we can claim that the film of PEG-OPE-rGO retained strong two-photon absorption in-

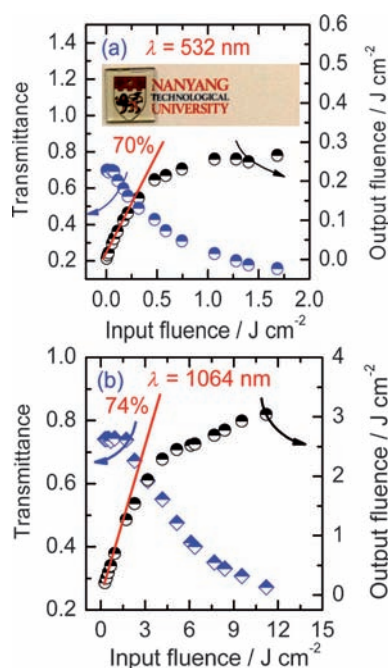


**Figure 4.** OL response and normalized nonlinear transmittance characteristics of PEG-OPE-rGO in PMMA under the excitation at (a) 532 nm and (b) 1064 nm. Inset in Figure 4a: photograph of film cast on glass.

duced OL response owing to the weaker NLS in solid films. To facilitate the comparison, the OL parameters of GO and PEG-OPE-rGO measured at 532 and 1064 nm are summarized in Table 1. It can be concluded that the PEG-OPE-rGO has better OL response than does the GO, no matter if it is dispersed in organic solvents or polymer films. Moreover, it is noteworthy that the PEG-OPE-rGO has the best OL performance compared to those hybrid materials previously reported.

$\lambda$ [nm]	Parameter [ $\text{J cm}^{-2}$ ]	GO		PEG-OPE-rGO		
		Ethanol	Ethanol	$\text{CHCl}_3$	$\text{CS}_2$	Solid film
532	threshold	1.19	0.75	0.35	0.31	0.65
532	onset	0.19	0.11	0.08	0.07	0.10
1064	threshold	10.32	4.80	3.52	3.50	6.50
1064	onset	1.36	0.80	0.54	0.54	1.25

## Conclusion

In conclusion, we report the broadband OL property of a novel amphiphilic graphene composite (PEG-OPE-rGO), within which rGO is noncovalently functionalized by an amphiphilic copolymer (PEG-OPE). The thresholds for the OL properties of the PEG-OPE-rGO composite, excited with 532 and 1064 nm nanosecond pulses, are much lower than those of the GO suspension, no matter if the composite is dissolved in polar or nonpolar solvents. Besides the nonlinear scattering mechanism which is common in nanostructured materials, the combination of multiphoton absorption and energy transfer also contribute

much to the enhancement of OL in PEG-OPE-rGO composite. Therefore, the noncovalently functionalized PEG-OPE-rGO is not only a promising OL material with broad temporal and spectrum responses, but also provides a standard for the further optimization of composites with other nonlinear optical chromophores to obtain designed OL materials.

## Experimental Section

The optical limiting (OL) properties for the noncovalently functionalized amphiphilic graphene composites at 532 and 1064 nm were measured by the fluence-dependent transmittance method under the excitation of 6 ns pulse with repetition of 10 Hz. The laser pulses were generated from a Q-switched Nd:YAG laser. The laser beam was focused into the solutions contained in a 1 cm length quartz cuvette. The spot sizes for 532 and 1064 nm were 26.7 and 34.7  $\mu\text{m}$ , respectively. The UV/Vis absorption spectra of solutions were recorded by the Shimadzu UV-3101 PC spectrophotometer. For the measurements of PL emission spectra, a continuous wave He-Cd laser emitting at 325 nm was used as the excitation source and the signals were dispersed by a 750 mm monochromator combined with suitable filters, and detected by a photomultiplier using the standard lock-in amplifier technique. Time-resolved PL (TRPL) spectra were carried out at room temperature by using the time-correlated single photon counting (TCSPC) technique, with a resolution of 10 ps (PicoQuant PicoHarp 300). The second harmonic of Titanium sapphire laser (Chameleon, Coherent Inc.) operating at 350 nm (100 fs, 80 MHz) was used as the excitation source.

## Acknowledgements

This study was supported by the Singapore Ministry of Education through the Academic Research Fund (Tier 1) under project no. RG63/10, the Singapore National Research Foundation through the Competitive Research Programme (CRP) under project no. NRF-CRP5-2009-04, the Singapore Ministry Of Education under AcRF Tier 2 (ARC 10/10, no. MOE2010-T2-1-060), the Singapore National Research Foundation under CREATE programme: Nanomaterials for Energy and Water Management, and the Nanyang Technological University under the start-up grant no. M4080865.070.706022.

**Keywords:** composites · graphene · nonlinear optics · polymers

- [1] K. Mansour, M. J. Soileau, E. W. Van Stryland, *J. Opt. Soc. Am. B* **1992**, *9*, 1100–1109.
- [2] J. E. Riggs, D. B. Walker, D. L. Carroll, Y. P. Sun, *J. Phys. Chem. B* **2000**, *104*, 7071–7076.
- [3] L. Vivien, E. Anglaret, D. Riehla, F. Bacoua, C. Journet, C. Goze, M. Andrieux, M. Brunet, F. Lafonta, P. Bernier, F. Hache, *Chem. Phys. Lett.* **1999**, *307*, 317–319.
- [4] L. W. Tutt, A. Kost, *Nature* **1992**, *356*, 225–256.
- [5] M. Calvete, G. Yang, M. Hanack, *Synth. Met.* **2004**, *141*, 231–243.
- [6] G. Lim, Z. Chen, J. Clark, R. G. S. Goh, W. Ng, H. Tan, R. H. Friend, P. K. H. Ho, L. Chua, *Nat. Photonics* **2011**, *5*, 554–560.
- [7] J. Wang, Y. Hernandez, M. Lotya, J. N. Coleman, W. J. Blau, *Adv. Mater.* **2009**, *21*, 2430–2435.
- [8] Y. Xu, Z. Liu, X. Zhang, Y. Wang, J. Tian, Y. Huang, Y. Ma, X. Zhang, Y. A. Chen, *Adv. Mater.* **2009**, *21*, 1275–1279.

- [9] J. Balapanuru, J. Yang, S. Xiao, Q. Bao, M. Jahan, L. Polavarapu, J. Wei, Q. Xu, K. Loh, *Angew. Chem.* **2010**, *122*, 6699–6703; *Angew. Chem. Int. Ed.* **2010**, *49*, 6549–6553.
- [10] Y. Liu, J. Zhou, X. Zhang, Z. Liu, X. Wan, J. Tian, T. Wang, Y. Chen, *Carbon* **2009**, *47*, 3113–3121.
- [11] Z. Liu, Y. Xu, X. Zhang, X. Zhang, Y. Chen, J. Tian, *J. Phys. Chem. B* **2009**, *113*, 9681–9686.
- [12] Y. Li, J. Zhu, Y. Chen, J. Zhang, J. Wang, B. Zhang, Y. He, W. J. Blau, *Nanotechnology* **2011**, *22*, 205704.
- [13] T. C. He, W. Wei, L. Ma, R. Chen, S. X. Wu, H. Zhang, Y. H. Yang, J. Ma, L. Huang, G. G. Gurzadyan, H. D. Sun, *Small* **2012**, DOI: 10.1002/sml.201200249.
- [14] P. P. Li, Y. Chen, J. Zhu, M. Feng, X. Zhuang, Y. Lin, H. Zhan, *Chem. Eur. J.* **2011**, *17*, 780–785.
- [15] a) Y. Xu, H. Bai, G. Lu, C. Li, G. Shi, *J. Am. Chem. Soc.* **2008**, *130*, 5856–5857; b) D. Lee, T. Kim, M. Lee, *Chem. Commun.* **2011**, *47*, 8259–8261.
- [16] X. Qi, K. Pu, H. Li, X. Zhou, S. Wu, Q. Fan, B. Liu, F. Boey, W. Huang, H. Zhang, *Angew. Chem.* **2010**, *122*, 9616–9619; *Angew. Chem. Int. Ed.* **2010**, *49*, 9426–9429.
- [17] S. Saxena, T. A. Tyson, S. Shukla, E. Negusse, H. Chen, J. Bai, *Appl. Phys. Lett.* **2011**, *99*, 013104–013105.
- [18] X. Huang, X. Y. Qi, F. Boey, H. Zhang, *Chem. Soc. Rev.* **2012**, *41*, 666–686.
- [19] X. Huang, Z. Yin, S. Wu, X. Qi, Q. He, Q. Zhang, Q. Yan, F. Boey, H. Zhang, *Small* **2011**, *7*, 1876–1902.
- [20] K. Susumu, J. A. N. Fisher, J. Zheng, D. N. Beratan, A. G. Yodh, M. J. Therien, *J. Phys. Chem. A* **2011**, *115*, 5525–5539.
- [21] J. Zhu, Y. Li, Y. Chen, J. Wang, B. Zhang, J. Zhang, W. J. Blau, *Carbon* **2011**, *49*, 1900–1905.
- [22] L. W. Tutt, T. F. Boggess, *Prog. Quantum Electron.* **1993**, *17*, 299–338.
- [23] G. S. He, J. Zhu, K. T. Yong, A. Baev, H. X. Cai, R. Hu, Y. Cui, X. H. Zhang, P. N. Prasad, *J. Phys. Chem. C* **2010**, *114*, 2853–2860.
- [24] J. Wang, W. J. Blau, *J. Opt. A Pure Appl. Opt.* **2009**, *11*, 024001.
- [25] H. A. Papazian, *J. Am. Chem. Soc.* **1986**, *108*, 3239–3241.
- [26] H. Wang, Z. Li, P. Shao, J. Qin, Z. Huang, *J. Phys. Chem. B* **2010**, *114*, 22–27.
- [27] a) M. Albota, D. Beljonne, J.-L. Brédas, J. E. Ehrlich, J.-Y. Fu, A. A. Heikal, S. E. Hess, T. Kogej, M. D. Levin, S. R. Marder, D. McCord-Maughon, J. W. Perry, H. Röckel, M. Rumi, G. Subramaniam, W. W. Webb, X.-L. Wu, C. Xu, *Science* **1998**, *281*, 1653–1656; b) D. Beljonne, W. Wenseleers, E. Zojer, Z. Shuai, H. Vogel, S. J. K. Pond, J. W. Perry, S. R. Marder, J. L. Brédas, *Adv. Funct. Mater.* **2002**, *12*, 631–641; c) K. Ogawa, A. Ohashi, Y. Kobuke, K. Kamada, K. Ohta, *J. Am. Chem. Soc.* **2003**, *125*, 13356–13357; d) M. Williams-Harry, A. Bhaskar, G. Ramakrishna, T. Goodson III, M. Imamura, A. Mawatari, K. Nakao, H. Enozawa, T. Nishinaga, M. Iyoda, *J. Am. Chem. Soc.* **2008**, *130*, 3252–3253.
- [28] a) J. R. Lakowicz, *Principles of Fluorescence Spectroscopy, 3rd Edition*, Springer, New York, **2006**; b) R. Chen, D. Li, B. Liu, Z. Peng, G. G. Gurzadyan, Q. Xiong, H. Sun, *Nano Lett.* **2010**, *10*, 4956–4961.
- [29] a) E. Mutlugün, S. Nizamoğlu, H. Volkan Demir, *Appl. Phys. Lett.* **2009**, *95*, 033106; b) C. Liu, Z. Wang, H. Jia, Z. Li, *Chem. Commun.* **2011**, *47*, 4661; c) H. Dong, W. Gao, F. Yan, H. Ji, H. Ju, *Anal. Chem.* **2010**, *82*, 5511; d) Y. Piao, F. Liu, T. S. Seo, *Chem. Commun.* **2011**, *47*, 12149.
- [30] Y. Zhou, Q. Bao, L. Tang, Y. Zhong, K. P. Loh, *Chem. Mater.* **2009**, *21*, 2950–2956.
- [31] B. Zhao, B. Cao, W. Zhou, D. Li, W. Zhao, *J. Phys. Chem. C* **2010**, *114*, 12517–12523.
- [32] a) M. Sheik-Bahae, A. A. Said, T. H. Wei, D. J. Haga, E. W. Van Stryland, *IEEE J. Quantum Electron.* **1990**, *26*, 760–769; b) M. Sheik-bahae, A. A. Said, E. W. Van Stryland, *Opt. Lett.* **1989**, *14*, 955–957.

---

Received: May 14, 2012

Published online on July 10, 2012